THE TECHNICAL UNIVERSITY OF KENYA

SCHOOL OF PHYSICS AND EARTH SCIENCES

DEPARTMENT OF TECHNICAL AND APPLIED PHYSICS

PROJECT PROPOSAL:
IDENTIFICATION OF ECLIPSING BINARY STAR SYSTEM DW CEP (OPTICAL ASTRONOMY - STAR LIGHT IN THE UNIVERSITY LAB - ASTROLAB PROJECT)

KARANJA STEPHEN CHEGE
SPPI/00596/2015

This project report is submitted in partial fulfillment of the requirement for the award of an academic degree in

BACHELOR OF TECHNOLOGY (TECHNICAL AND APPLIED PHYSICS)

NOVEMBER 2020

DECLARATION

I declare that this fourth year project proposal is my original work and has not been submitted elsewhere for examination, award of an academic degree or for publication. Where other people’s work or my own work has been used, this has properly been acknowledged.

Karanja Stephen Chege Sign: ________

This thesis has been submitted with our approval as university supervisors for the degree of Technical and Applied Physics

Prof. Paul Baki Sign: _________

Mr. Calvince Juma Sign: __________

DEDICATION

This project is dedicated to my family and friends who have been there for me.
May God bless you abundantly.

ACKNOWLEDGMENT

I would like to thank the Almighty God for giving me the strength and perseverance throughout this project.

I would also like to extend my sincere gratitude to my supervisors Prof. Paul Baki and Mr. Calvince Juma for their guidance, recommendations and encouragements throughout this project.

My sincere gratitude to one Dr. Michelle Gerbaldi for her insightful ideas and guidance in this project.

I extend my sincere gratitude to the entire fraternity of The Technical University of Kenya for offering a suitable and sound environment and facilities that enabled me to successfully complete my project.

I would like to acknowledge the Astronomy project group, for their motivation and criticism throughout this project.

ABSTRACT

Observations done indicate that majority of stars are clustered together as viewed on the celestial sphere from the Earth but when viewed with powerful telescopes we realize that they are two or more stars revolving around their barycentres. The barycentre is the center of mass of two or more bodies that orbit one another. Most stars are usually in groups from binary systems to globular clusters which composes of hundreds of thousands of stars. In binary systems, stars move in elliptical orbit with respect to their barycentre.

In this project, we identified a binary star system through the CDS (Centre de Données astronomiques de Strasbourg - Strasbourg astronomical Data Center) website (http://cds.u-strasbg.fr/). In this case, the star DW Cep was the subject of the study. We then used a robotic 40mm telescope based in the Canary Island, Spain (*Teide Observatory*) to obtain both raw and reduced images - in the format (.fits.fz). The telescope was accessed through the Las Cumbres Observatory website (https://observe.lco.global/).

Aladin sky atlas was then used to map out the comparison stars that will help us obtain the light curve since they had a constant magnitude. This was followed by running the data through SAOImage DS9 which we used to reduce the data to 16 bit integer. Iris software requires that the image files not have an intensity larger than 32767 pixels. Iris was used to attain the intensity or brightness values of the variable and comparison stars. From that data, we plotted a light curve that showed the secondary and the primary eclipse. The light curves plotted included the differential magnitudes against the Julian date of the observation and the differential magnitude against the phase of the star system. These light curves provided us with the information necessary to determine whether the selected target is an eclipsing binary star, the orbital period and the linear size of the star system.

Table of Contents

LIST OF ABBREVIATIONS

JD – Julian Dates
CCD – Charged Coupled Device
mas – milliarcsec
AU – Astronomical Units
NASA – National Aeronautics and Space Administration
RA – Right Ascension
Dec – Declination
T – Observation time
T_0 - Epoch time
P – Period (orbital period)
G – Gravitational constant

CHAPTER 1: INTRODUCTION

One of the most useful scientific research projects suitable for small telescopes equipped with CCD cameras or high-quality photometers is monitoring period changes in short-period binaries. The Charge Coupled Devices (CCD) are preferred over photo-multiplier tubes and photo-diodes because they are very sensitive to light over a wide range of wavelengths from the ultraviolet to infrared and can measure many stars at once in contrast to photo-multiplier tubes and photo-diodes that measure one star at a time. Many such binaries are bright ($V<12$), have orbital periods less than one day and have deep eclipse minima ($V>0.1$), making them easily observable.

Binary stars are important because they are numerous in number and we can extract more information about stars by comparing them among themselves and are also the only source of our knowledge on the basic characteristics of stars and their formation. This gives us a greater understanding of the evolution of the universe, it's apparent size, it's age and the expansion rate. Binary stars are also ideal distance estimators since absolute magnitudes of the components can be readily obtained from their luminosity. The figure below shows a binary star system:

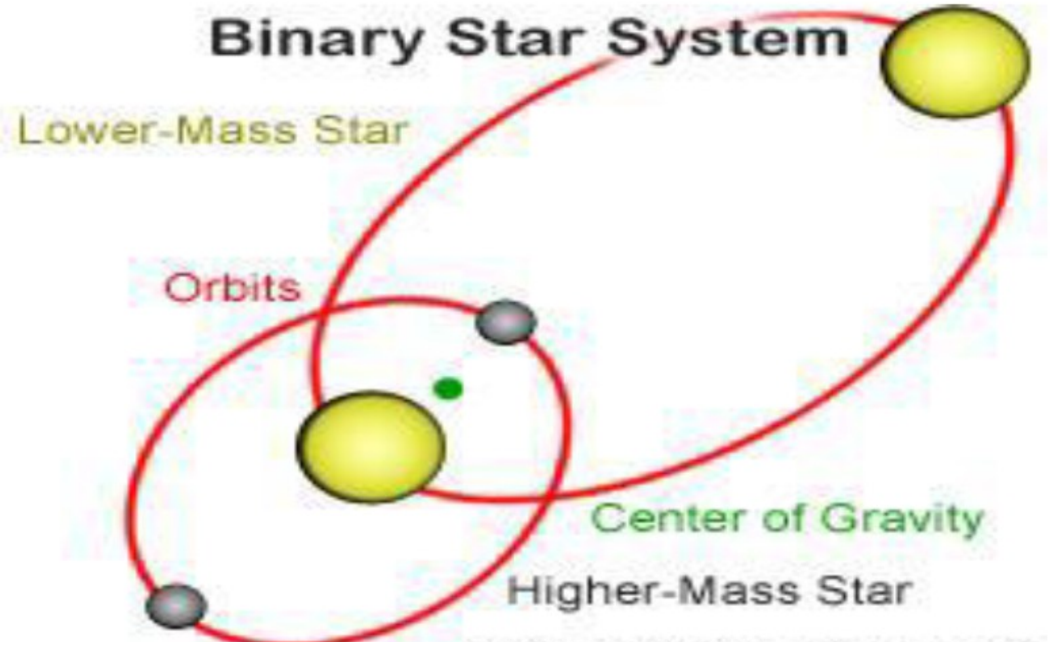

Figure 1.0: A binary star system

There are various types of binary stars namely:

- **Optical double stars:** they appear close together just by coincidence since they lie along the same line of sight but they are not true binaries and could be light years away from each other. They are not gravitationally bound and are totally independent of each other.
- **Astrometric binary stars:** this a binary system where one of the companion is too bright hence it dominates the other faint companion. Such binaries cannot be observed using a telescope hence they are not visual binaries. We detect the companion of the bright star by using astrometry which measures and explains the positions and movements of stars and other celestial bodies. If only one star is present, it moves on a straight line. But in binary or multiple system the orbital motion is different. The unseen companion is implied by the oscillatory motion of the observed element of system.
- **Spectroscopic binaries:** In this case the stars are so close to one another that even with a high-resolution telescope, we are unable to observe both members directly. We can detect the presence of the binary system via the Doppler effect that is evident in the periodic shift in spectral lines of the stars or the observed flux.
- **Eclipsing binaries:** If the line of sight of the observer lies close to the orbital plane of the system we can witness eclipses. Some of the light is blocked as one component passes in front of the other, the observed flux is diminished. Such a time-dependent change in flux enables us to further constrain the physical parameters of binary system. Eclipses can be used to obtain the inclination, stellar masses, radii, orbital eccentricity, effective temperatures. Eclipsing binary systems could also be spectroscopic or astrometric system at the same time if we can see eclipses.

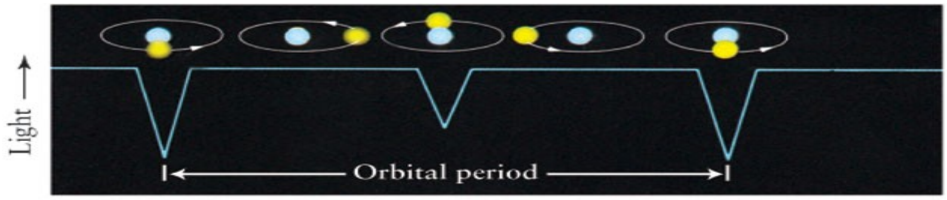

(a) Partial eclipse

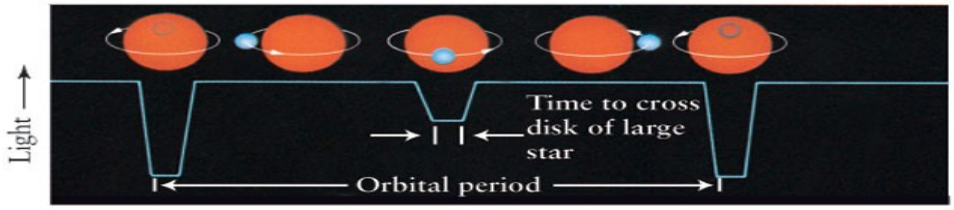

(b) Total eclipse

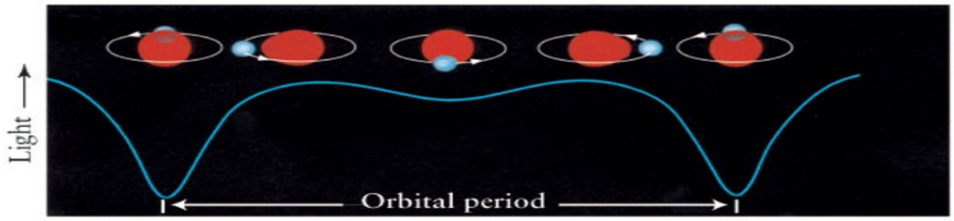

(c) Tidal distortion

Figure 1.1: An Eclipsing binary star system

In most cases, the binary stars are not of the same size, luminosity and type. During the phase where the smaller star moves in front of the larger one, the hidden region emits light that does not reach observers on Earth. Among astronomers, this phase in the star system is known as a primary minimum. The brightness curve can however record another type of minimum – a secondary minimum. When the smaller star moves behind the larger star, the luminosity drops, and is usually significantly lower as compared to the phases where the two stars are next to each other. The difference in brightness between the two stars is the factor that determines whether the primary minimum or the secondary minimum is the lowest one.

When the small star has a surface brightness that is lower than that of its companion star, the primary minimum is lower. Likewise, the secondary minimum becomes quite obvious on the brightness curve if the larger star is the darker of the two.
The brightness curve not only determines which of the two minimums is lower, but it also provides us with necessary information about the system itself, such as the relationship between the radii of the two stars, the period of their individual orbits and the mass of each of the components.

1.1 Statement of the Problem

The Earth is a very small stage in a vast cosmic arena, even these stars, which seem so numerous, are as dust - in the enormity of the space in which there is nothing. This challenges us to study stars more hence the need to know more about them.
When we look up at night and view the stars, everything we see is shinning irregardless of the vast distances separating us from them. When we look at them it becomes hard to tell whether they are optical doubles (line-of-sight alignment of two unrelated stars at different distances but observed together from the Earth).For ages, it has been a problem to distinguish binary stars that are bound to each other by gravity from optical double stars which are not bound together and have no physical connection.

It is also a challenge to acquire information such as the masses, volume, temperatures, luminosity, radii and photospheric composition which cannot be clearly defined from observing a single star. In recent years, studies done on binary eclipsing systems have mainly adopted the differential magnitude method. This project also aims to use a new method. This is the use of the phase of the stars acquire the required results.

1.2 Problem Justification

There is a need for a close and detailed study of binary star so as to distinguish them from those that coincidentally appear together since they lie on a continuous line of sight. This will help eliminate illogical assumptions about the type of stars seen by observers.

Accurate identification of binary stars will help in obtaining more detailed data about stars such as their masses, volume, temperatures, luminosity, radii and chemical composition which could not be obtained earlier from observing single stars.
This will help us know how other heavenly bodies affect us especially the stars.
The knowledge obtained from such studies can help us to come up with more advanced theories on the evolution of our universe and keep astronomers on the competitive edge of new discoveries.

1.3 Main Objective

The main objective of this project is to be able to analyze data obtained to estimate the period of the binary star system and calculate the diameter of the primary star.

1.4 Specific Objectives

The specific objectives of the project are to:

- Select an eclipsing binary system.
- Data acquisition for the star system from the Las Cumbres Observatory.
- Analyze the data using several software by reducing it and enhancing it to formats easier to understand and interpret.
- Measure the brightness of the system in order to obtain a light curve over one orbital phase.
- Calculate the estimates of the stars orbital period and the diameter of the primary star.

CHAPTER 2: LITERATURE REVIEW

On 28th October 2010, an article *A two-solar-mass neutron star measured using Shapiro delay* (1) was published in International weekly journal of science. The Shapiro delay is the extra time delay light experiences by traveling past a massive object due to general relativistic time dilation. It was first verified by Irwin Shapiro in 1964. In binary pulsar systems that we see it nearly edge-on, excess delay in the pulse arrival times can be observed when the pulsar is situated nearly behind the companion during orbital conjunction. As described by general relativity, the two physical parameters that characterize the Shapiro delay are the companion mass and inclination angle.
The authors studied pulsar and its binary companion nearly edge-on.

Pulsars are supernova remnants and so far more than 1500 pulsars have been discovered. A pulsar is a rotating neutron star that have jets of particles moving almost at the speed of light streaming out above their magnetic poles. These jets produce very powerful beams of light, that we can detect on Earth. A neutron star is about 20 km in diameter and has the mass of about 1.4 times that of our Sun, thus they are very dense. Its internal temperature is to 108 K and surface temperature around 106 K. Composition and properties of neutron star are still theoretically uncertain. Like we saw in previously, we are able to measure mass and other parameters of a star when it is in a binary system. Some of the important parameters published in article are presented in the next table:

Parameters	***Value***
Pulsar's spin period	*3.1508 ms*
Orbital period	*8.6866 days*
Inclination	*89.17°*
Mass pulsar	*1.97* $M_{\odot}$
Mass companion	*0.50* $M_{\odot}$
Characteristic age	*5.2 Giga-year*

These measurements are very accurate and a pulsar mass is by far the highest precisely measured neutron star mass determined so far. Because the mass of pulsar is much more than it supposed to be, the density is higher and they can more precisely determine or rule out theoretical models of their composition.

In October 2009 an article: *Accurate masses and radii of normal stars: modern results and applications* (2) was published. The authors identified 95 detached binaries containing 190 stars (α Centauri and 94 eclipsing systems), consistent with the criteria that they had to be non-interacting systems and their masses and radii can both be trusted to be accurate to better than ±3%. They searched the literature for such systems, examined and recomputed all data. For each system they determined the distance, eccentricity, period and approximate age, and for most members, their rotational velocities, metallic abundances, masses, radii, luminosity, magnitudes and effective temperatures. The effective temperature is accurate to ±2%, distance to ±5% and age to 25 to 50%. Later on it is revealed how the physical parameters affect stellar evolution.

Kepler satellite was launched in March 2009. The Kepler Mission is a NASA Discovery Program for detecting potentially life-supporting planets around other stars and determine how many of the billions of stars in our galaxy have such planets. This is done by photometry. Observations have already shown the presence of planets orbiting individual stars in multiple star systems. The resolution needed to detect transit of the planet must be very high and Kepler telescope simultaneously measures the variations in the brightness of more than 100,000 stars every 30 minutes, so there is a lot of data to examine. From these data certain physical parameters for eclipsing binaries can be extracted.

John Mitchell in 1767 proposed that double stars were physically connected to each other. He argued that the probability of two stars being aligned close together by chance was much smaller than the recorded pairs (5). William Herschel published a catalogue of 269 double stars in 1782 and a further 434 two years later. After continuous observations of the recorded double stars, by 1803, he was able to prove that some of the pairs had a mutual physical attraction that could not be explained by differential parallaxes. By the end of the 19th century, E. C. Pickering had discovered the first spectroscopic binaries. His discovery revealed that each of the two components of the Mizar system contained two stars making it a quadruple system (3). The first eclipsing binary star, Algol, was also confirmed as a spectroscopic binary in 1889 (4).

There has been many theories on the formation of binary stars. The three most popular ones include the capture theory, the binary fission hypothesis and fragmentation theory.

The capture theory was hypothesized in 1867 by an Irish physicist, G. J. Stoney. He proposed that the two companion stars were initially single stars, independent of each other. As they approached each other, they were forced to revolve around the other about a central center of gravity (10). This theory however, has been disregarded as a source of energy dissipation is required to restrain the two stars together (11). There exists three different cases within the capture theory in which the formation of binary stars can occur. The first process is when a third-body is present. The energy dissipated from the two stars orbit is propagated to the third star as kinetic energy. This energy pushes the third star out of the system while the other two become gravitationally bound (12). This model has a high chance of occurrence in a region of high stellar density such as the center of a globular cluster making the three-body capture model a rare occurrence and usually creates binary systems that are both massive and very wide apart (11). The second process is tidal dissipation through two-body dissipation. These two-body interactions occur more often than the three-body interactions. For this process to successfully happen the two bodies must be close enough to dissipate energy to bind the system (13). The excitation of the tides in the stars converts the orbital energy into heat. In cases were the tides are not significant because the distance is not close enough, many counters are needed to dissipate enough energy (12). The third case occurs when there is an interaction with the gaseous disks of a rotating protostar. (14). A protostar is an early phase in star formation that forms by the gas of giant molecular cloud contracting (7). If two protostar disks undergo a close interaction the gases can cause dissipation through certain processes such as gravitational drag, gas drag, tidal forces, radiation and shock heating. Binary stars formed in this method would have separations limited to the size of the protostellar disks, around 10 – 100 AU (11). As these three processes depend on many variables and must occur in areas of high stellar density clusters, the capture method cannot be the dominant process in the creation of the majority of binaries (12).

The Binary Fission Hypothesis has been around for a long time and was once thought to be the most likely candidate (15). As the star accumulates materials during the protostar phase or after disk accretion is completed and it begins contracting towards the main sequence fission occurs. The law of conservation of angular momentum means that as it contracts the star must increase its spin (14). It is then said to have become rotationally unstable as the ratio of gravitational to rotational energy becomes higher. As the ratio increases, the gas cloud evolves taking an ellipsoidal shape and becoming progressively distorted (16). As the distortion grows, a bar shape is formed and then proceeds to take the form of a bar-bell. A star is then formed with the accumulated masses at the end of the barbell, creating a contact binary. As they move towards the main sequence, they become detached (17). Simulations have however ruled out this method because the spiral arms of the system and the gravitational torque are able to eject the mass and angular momentum. The result is still considered fission as there is break up of component material. A disk around stellar remnant is created as a result of the ejected mass (18).

The Fragmentation theory is currently the leading theory for the formation of binary stars. It suggests that binary stars are created during the collapse of a molecular cloud to create a protostar. A protostar usually collapses in two phases. The first is an early optically thin isothermal phase that is followed by an optically thick adiabatic phase. The conditions during the isothermal phase are more favorable for fragmentation to occur (14). As fragmentation is a relatively new theory, there are several differing ideas on how it works. One of the hypothesis is that the rotating collapse of material from the in-falling envelope induces fragmentation (12). During the collapse, the density of the spherical envelope increases. A large, flattened asymmetric structure with double density peaks is formed from the rotation. Wide binary systems with a separation distance of approximately 1000 AU or close binary systems with less than half that distance are created as a result of the angular momentum of the in-falling which affects the separation of the peaks (19). The second hypothesis suggests that the disks of a protostar when subjected to a strong gravitational instability, may fragment to create one or more companions (20). The angular momentum of the in-falling envelope forms a massive disk. The gravity of the disk allows fragmentation to occur at large radii therefore creating binary components. These new fragments would be in the same plane as the original star and would have a common angular momentum vector. This second method is considered to be the most likely fragmentation mechanism for creating binary stars after recent research as shown by J. J. Tobin et al (19). Using observations from the Very Larger Array (VLA) and the Combined Array for Research in Millimeter-wave Astronomy (CARMA) it was discovered that an apparent circumbinary disk exists around two protostars $_{\text{e.g.}}$ L1165-SMM1. Two protostars were also observed to have secondary sources located almost orthogonal to the outflow direction, which would be expected if their formation occurred within the disk and the outflow is perpendicular to the equatorial plane. These results along with other recent data makes disk fragmentation the strongest theory on the formation of close binary stars.

In the majority of binary systems, the two companion stars are sufficiently far away such that they have a negligible effect on each other. Their evolution happens independently much like single stars with only a slight force of gravity keeping them bound (1). However, when binary stars are close enough they can alter the structure of one another. The surface of the secondary star can be distorted by the primary companion through the gravitational force being much stronger at its nearest side than its farthest creating a pear-like shape. This is called a tidal effect. This distortion causes a loss of the total internal energy. As the stars rotate, material is shifted into the swelled region and these materials create friction by rubbing against each other. This causes a loss of rotational and orbital energies resulting in the circularization of the orbits, and causes the stars to always face the same direction as one another. At this point, the spins become synchronized (7). The distorted star might also lose some of its outer layers to its companion if the force is strong enough (1).

CHAPTER 3: DESIGN AND METHODOLOGY

3.1 Choice of Target

Factors to consider in selection of target

- The orbital period should allow observation of various phases of the period for several times in a month. About 2 days to allow for acquisition of up to 15 images in a month.
- The period of the target should not be too close so as to avoid very close observations in the same phase.
- For better observation of the target the primary eclipse should be about 10% of the total period

Visibility of the target

- We consider to choose a target that is visible for a wide fraction of the night by choosing a suitable range of the right ascension (RA) and declination (DE). We indicate this range in the constraints in the modified catalog.
- The declination should be positive and slightly negative (e.g -20^0 up to $+90^0$) for the observations done in the northern hemisphere but negative and slightly positive (-90^0 up to -20^0).
- The magnitude of our target should be in a range where it is not too faint and not too bright to saturate the field ($9.0 < V > 12.0$).

STARALT is a free online software that can be access through the link: http://catserver.ing.iac.es/staralt/. It is used to check the visibility of the target during the selected observation dates.
The information required to check the visibility of the target includes:
- The date of observation (calendar date).
- The name of the observatory.
- The coordinates of the observatory.
- The altitude and the off-set time at the observatory.
- The coordinates of the target.

The output of the STARALT query is shown in the graph below:

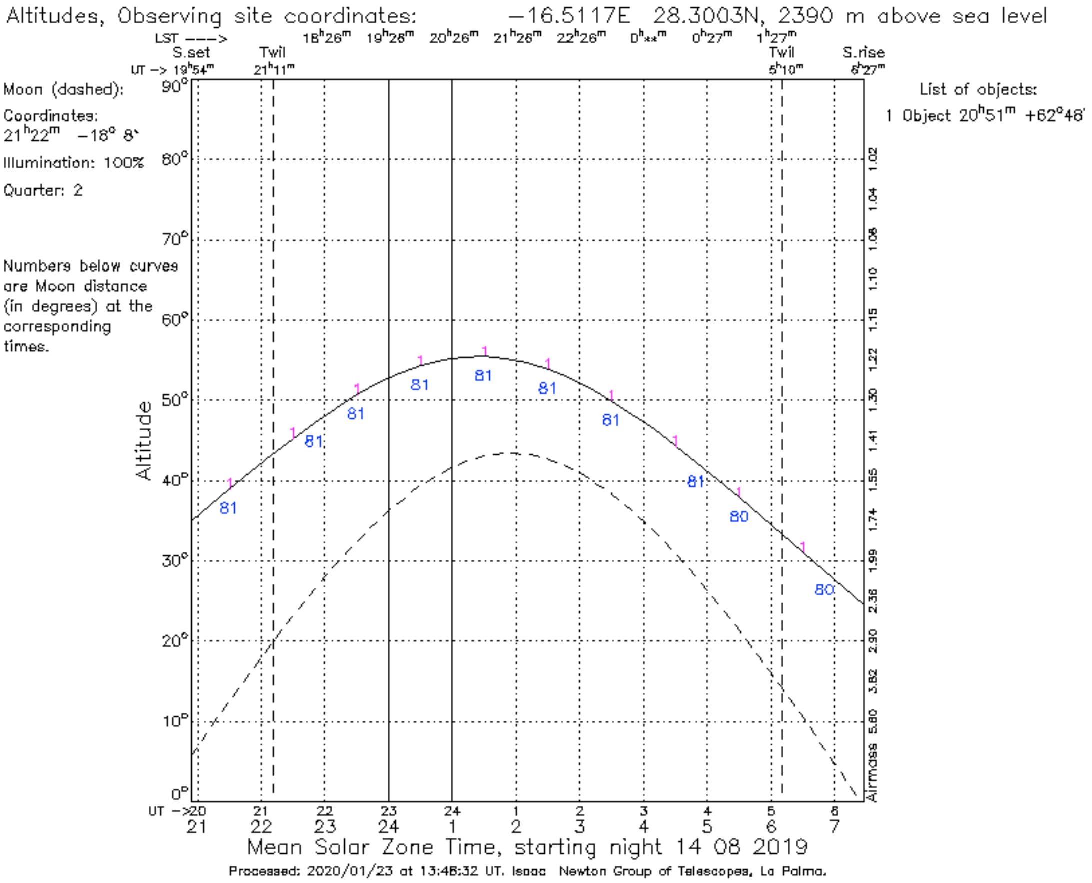

Figure 1.2: STARALT output

The angular distance between the Moon and the target is approximately 81 and the Moon is at 100% illumination.
Since the angular distance should be at least 60 and the air mass at least 1.04.

We will use the VizieR database developed at CDS (Strasbourg Data Center), to select a target in the following steps:

3.2 Selection of a Catalogue:

- Access CDS (Strasbourg Data Center) website via the URL (http://cds.u-strasbg.fr/) in the browser and then in the home page click on >> **VizieR Catalogue database**. (See Fig 1)
- To select the catalogue, go to the window >>**Astronomy** and scroll to >>**Binaries: eclipsing** and then we'll click on it to be highlighted.
- Click on >>**Find catalogs.** (See Fig 2)

- Click on >>**Get the Full list of 609 matching catalogs.** (See Fig 3)
- Scroll down and click on the journal containing information eclipsing binary stars >>**J/A+A/446/785** in the first column. (See Fig 4)

(J – Journal, **A+A –** Astronomy and Astrophysics, Volume **446**, Page **785)**

Selecting an Eclipsing Binary in the Catalogue:

- After clicking on the name of the journal >>**J/A+A/446/785** we will access the query of the catalogue.
- We will then modify the query by inserting constraints so as to get a limited number of targets depending on the factors considered when selecting the target and then click on >>**submit**.
- We will then acquire a list with a limited number of targets and the target with constraints closest to our requirements will be selected.

The constraints to be selected include the magnitude of the star at maximum brightness, depth of the primary minimum, duration of the primary eclipse and the coordinates of the range in which the target should lie within. The coordinates are carefully chosen depending on the time of the year. (See Fig 5)

3.3 Collecting Data from Las Cumbres Observatory Website:

- We will first visit their official website (https://lco.global/).
- Click on >>**Observing Portal**.
- On the next page we will key in the email address and password to login into our account to access the observing portal.
- Once the next page displays, click on >>**Submit observation**.
- On the next page, on the **General Information** tab, click on >>**Name** and input the name e.g Karanja_DW Cep.
- Click on >>**Proposal** and select >> **Astrolab – Starlight in the university lab LCOEPO2018A-001**.
- In the request tab, click on >>**Instrument** and select >>**0.4 meter sBIG**
- In the same tab, go to the configuration window. Click the >>**Exposure count** and input value as 1.
- Click on the >>**Exposure time** and input a value between 25 and 40. Any value lower than 25 will be too dark for accurate measurements and any value larger than 40 will be too bright for accurate measurement.
- Click on >>**Filter** and select blue.
- On the target tab, click on >>**Name** and input the name of the target star.

- Click on >>**right ascension** and input the right ascension coordinates of the target star.
- Click on >>**declination** and input the declination coordinates of the target star.
- On the right side of the page, click on >>**save draft** and the >>**submit request.** (See Fig 6)
- A pop-up page will then appear asking you to confirm the request and providing time on how long the observation will occur. Click on >>**agree.**
- Return to >>**home.** The request is successful if the request shows pending, indicating it’s awaiting telescope time.
- Once the request is complete, click on the name that was input for the request and this will take us to another page so that we can download the data.
- Click on the tab >>**Data** and select the reduced data with the file extension *.fits.fz* and click >>**Download selected.**
- The data will automatically download to your system. (See Fig 7)

3.4 Identification Of Comparison Stars:

In order to produce a light curve, we will need to observe comparison stars as well. A comparison star is a star used as a reference point in the determination of another star's position, brightness among other observable characteristics. They must be non-variable stars and located in the same field of view as the variable target. These are stars of known magnitude, ideally with similar magnitudes to the variable star. The comparison stars will be used to calibrate the magnitude of the variable star when reducing the data. During data reduction process, we will have to identify using star patterns the target and the reference ones. We will use two main software for star identification:

- Aladin Sky Atlas
- SAOImage DS9

The comparison stars chosen are:

BD+62 1865	**RA 20 52 17.67065, Dec +62 45 35.2740**
TYC 4251-1751-1	**RA 20 51 32.57642, Dec +62 44 23.9463**
TYC 4250-1321-1	**RA 20 50 54.52655, Dec +62 46 33.4799**

Aladin Sky Atlas

- We will then launch the Aladin Atlas application on the computer.
- Click on >>**file** and then on >>**Open server selector**.
- When the next page appears, we will click on >>**DSS…** and then select >>**DSS** from ESO (Garching/Deutschland – DSS.ESO).
- After the next page appears, in the Target space, we will input the the right ascension and declination of our target star. In the Sky Survey space we will select “DSS2-blue – POSSZUKSTU_blue”, then fill the Width (arcmin) and Height

(arcmin) spaces with 40 each. This will indicate the dimensions of the telescope, then click on >>**submit**.

- Go back to the previous page and then we will click on >>**SIMBAD** and then select >>**star** in the display filter and then click >>**submit**.
- The target star will then be displayed in the next page.
- We will then realign it so that we can be able to view more number of comparison stars easily.
- Once the comparison stars have been identified, we will plot a chart by connecting the stars by lines. These lines create a pattern that will be used to identify the position of both the target star and comparison stars. (See Fig 8)

3.5 Data Processing

3.5.1 SAOImage DS9

SAOImage DS9 is an open source,image processing software. The purpose of this step is to ensure the images are coded on 16-bit integer data so that the dynamic of a classical image is between 0-32767.

- Go to **>>menu bar >> File >> Open**. A new navigation window will open.
- Select the directory that contains the images in the *.fits* format **>>Enter**.
- When the image has been loaded, go to the **>>menu bar >> Scale >> Z scale**.
- Go to **>>menu bar >>Edit >>Rotate**. This step is used to rotate the image in the North Up direction so that it is easier to acquire the comparison stars from the pattern derived using the Aladin sky atlas. (See Fig 9)
- Go to **>>menu bar** and select **>>Region**. Drag the mouse on the target and draw a circle by holding down on the right button.
- Go to **>>menu bar >>Region >>Get Info**.
- A new window will appear and on it, click **>>Analysis** and the select on **>>Statistics**.
- Another window appears from which we will check the max value so that it is not above 32767 as discussed above.
- Go to **>>menu bar >>File >> Save**.
- Go to **>>menu bar >>File >>Display Header** and check the bits per pixel of the image. (See Fig 10)

This process is repeated for all the images to ensure that the data is correct.

3.5.2 IRIS Software

IRIS is a free astronomical images processing software. It uses images in both 16 and 32 bit integers as long as the max intensity of the targets does not exceed 32767 pixels. However, images of the file format *.fits* are not processed by the software. This means that all the files have to be manually changed to *.fit.*

- IRIS software will be installed into the computer from the website (http://www.astrosurf.com/buil/us/iris/iris.html).
- Once the installation process is complete, launch by double-clicking on the logo displayed on the desktop.
- Once it starts, two windows will be displayed, the main window and the threshold window.
- Go to >>**menu bar >>File menu >>Settings.**
- Once the settings dialog box is open, we will select the working path in which the images to be analyzed have been saved, click on the *.fit* format file and click on >>**OK**.
- Go to >>**menu bar >>Load >>Open** to bring the image to the main window. The image may not be seen due to the threshold limits and will be controlled automatically by clicking >>**Auto** on the floating threshold filter to set the black level and clipping level.
- We will then go to >> **menu bar >>File >>Image info**. A pop-up window will appear showing the information about the image.
- To save the output file, go to >>**File** >>S**ave** under the format **dat* and give it any name. The output file will be saved in the working directory that is being used.
- Drag the mouse around the target star and right click, select on **>>PSF.** This gives the quality of the image. On the new dialog box, x and y represent the coordinates of the target on the image. I represents the intensity of both the star and the sky background. It does not however represent the peak intensity but the sum of the intensities of the pixels forming the star, B represents the local sky background and FWHM X and Y represent the full width at half maximum of the star at axis X and Y respectively. Save the information so that the value of FWHM will be used when computing the aperture photometry of the target.
- Go to **>>menu bar >>Analysis >>Select Objects**. A mouse pointer with four arrows appears. Drag the mouse pointer and click on the target star followed by the comparison stars.
- Go to **>>menu bar >> Analysis >> Automatic Photometry.**
- On the automatic photometry window, change the input generic name to "*file-1-*" and in the number input box a value of "1" is selected.
- Click on the magnitude output to activate it and leave the magnitude constant value as 0.000

- Select >>**Aperture photometry.** The FWHM value then comes into play. It is doubled and the value put into the box. When complete click on >>**OK.**
- An output dialog box appears. Click on >>**File** >>**Save as** >> and save the file as a *.dat* file. The output window displays the magnitudes of the selected objects and the Julian date of the image file. (See Fig 11)
- This process is repeated for all the files.

3.6 COMPUTATION USING EXCEL AND PYTHON

The saved .**dat* files are then loaded on an excel sheet by using the separator as a blank. All the magnitudes and their corresponding Julian Dates are then added to another excel file.(See Fig 12) This is done so that we can compute the values of the differential magnitudes. This is done by subtracting the magnitude value of the comparison star from the variable star. This is done for all the comparison stars. The value of each comparison star is also subtracted form the other comparison $_{\text{i.e}}$ C1-C2, C2-C3, C3-C4...$_{\text{etc}}$(See Fig 13).

We will also require to compute the phase. This is done by selecting an epoch. An epoch is a date or referral time that marks the beginning of an astronomical event. The epoch chosen was that of the first day of the observations and is denoted by T_0.
The phase was calculated by subtracting the value of T_0 from the continuous Julian dates of the other images and the divided by the period of the system. ($T – T_0$ / P).
The phase is the fractional part of the solutions.
Traditionally, researchers have used the differential magnitude and Julian dates to plot graphs. We will use both the traditional method and the phase against differential magnitudes to obtain the required graphs. The graphs were plotted using both excel and python.

CHAPTER 4: RESULTS AND ANALYSIS

4.1 Analysis

After acquiring the data from the LCO telescopes, FITS files were used to compare the star patterns in SAOImage DS9 and Aladin. After the identification of the comparison stars and the variable, the brightness was measured using IRIS. The data was then tabulated on an excel spreadsheet. See figure 12 and 13. Figure 12 shows brightness levels for the variable and comparison stars, Julian dates of the observations and the phase. The magnitude of the variable star was deducted from the comparison stars. Figure 13 shows the differential magnitudes of the stars. Using the Epoch time, $T_{0,}$ as 2447392.36, dated 18th August 1988, the phase was calculated as:

$$\text{Phase} = \frac{(T - T_0)}{P}$$

where; T – Julian date

T_0 – Epoch time

P – orbital period

Once the phase value is acquired, only the fractional part is used (range from 0.0 – 1.0).

4.2 Results

The excel data was saved as a *.csv* file. The file was the uploaded to a jupyter notebook page by running a python code that generated the graphs for all the uploads and saved them to the working directory. The graphs were also plotted using excel. From the display header from the SAOImage DS9, we get that the star has a parallax of 0.0012131 mas. The parallax is the apparent displacement of an object because of a change in the observers point of view.

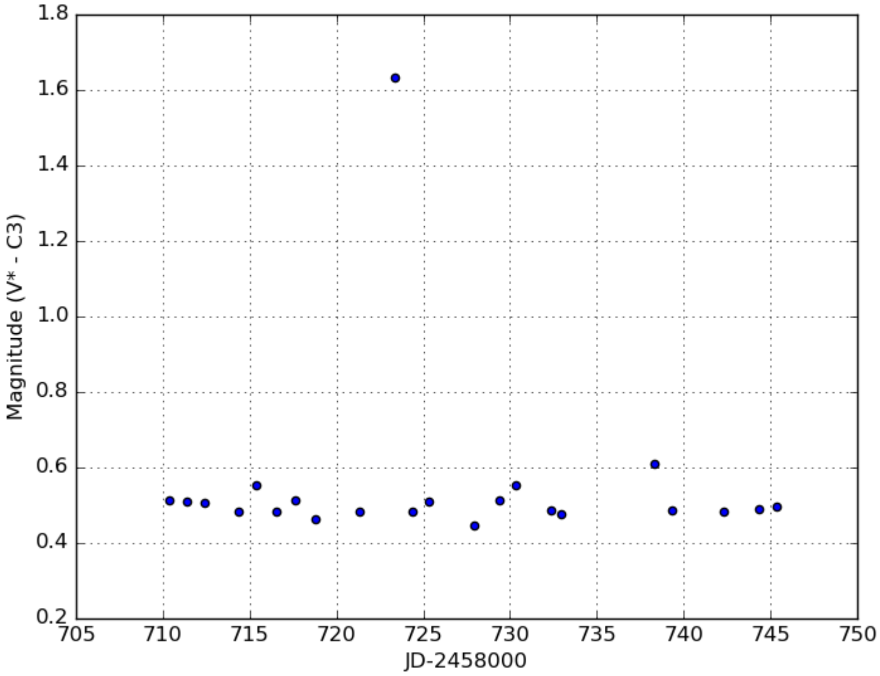

*Fig 1.3 Differential magnitude(V*C3) vs Julian Dates*

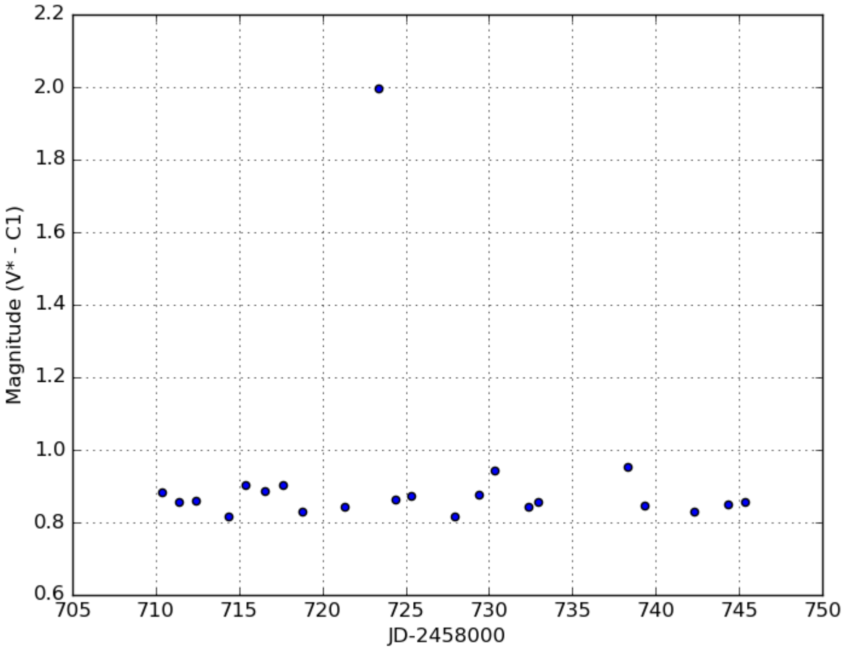

*Fig 1.4 Differential magnitude (V*C1) vs Julian Dates*

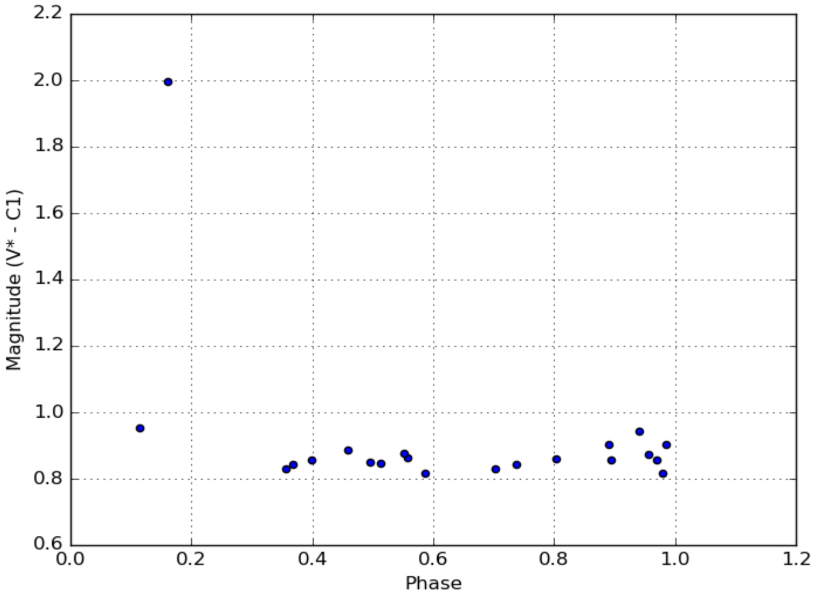

*Fig 1.4 Differential magnitude (V*C1) vs Phase*

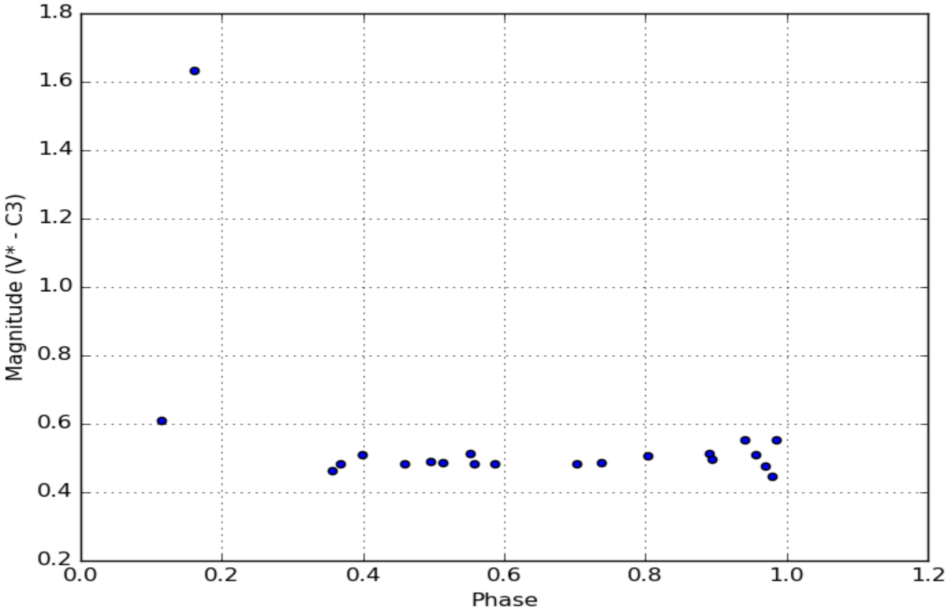

*Fig 1.4 Differential magnitude (V*C3) vs Phase*

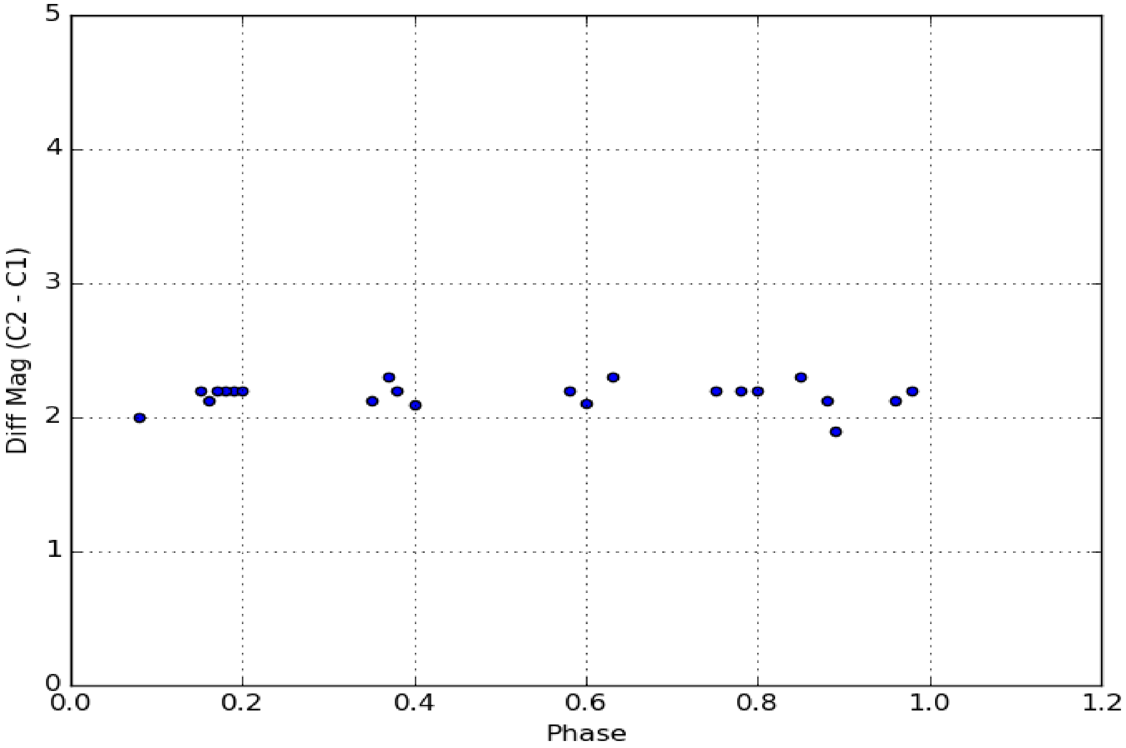

Fig 1.5: Light curve of C2-C1 differential magnitude against phase

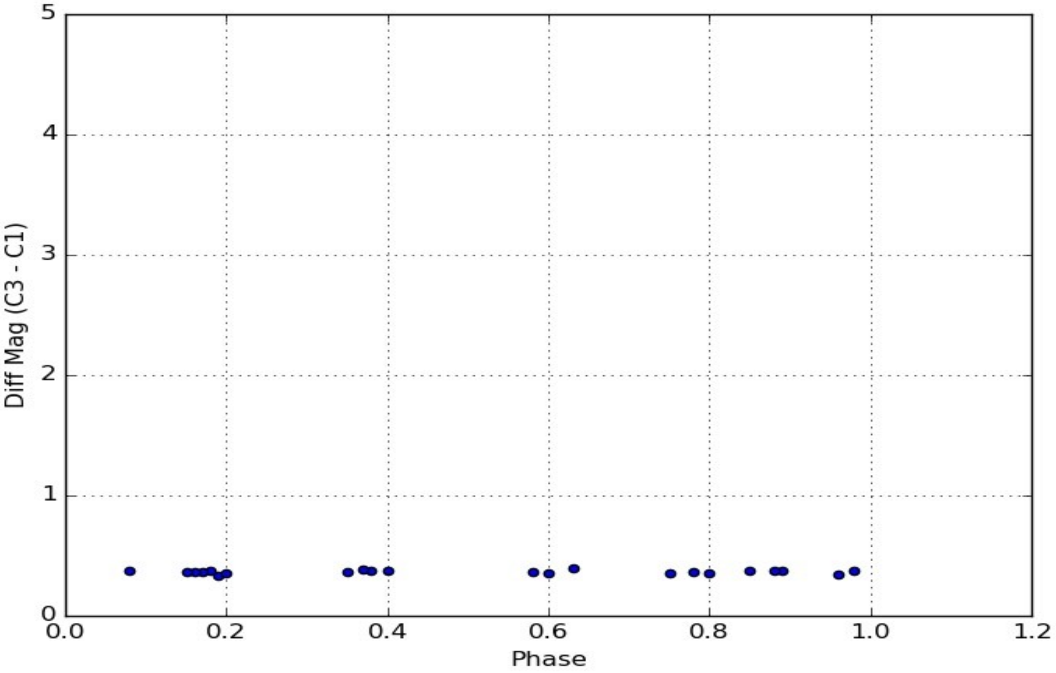

Fig 1.6 :Light curve of C3-C1 differential magnitudes against phase

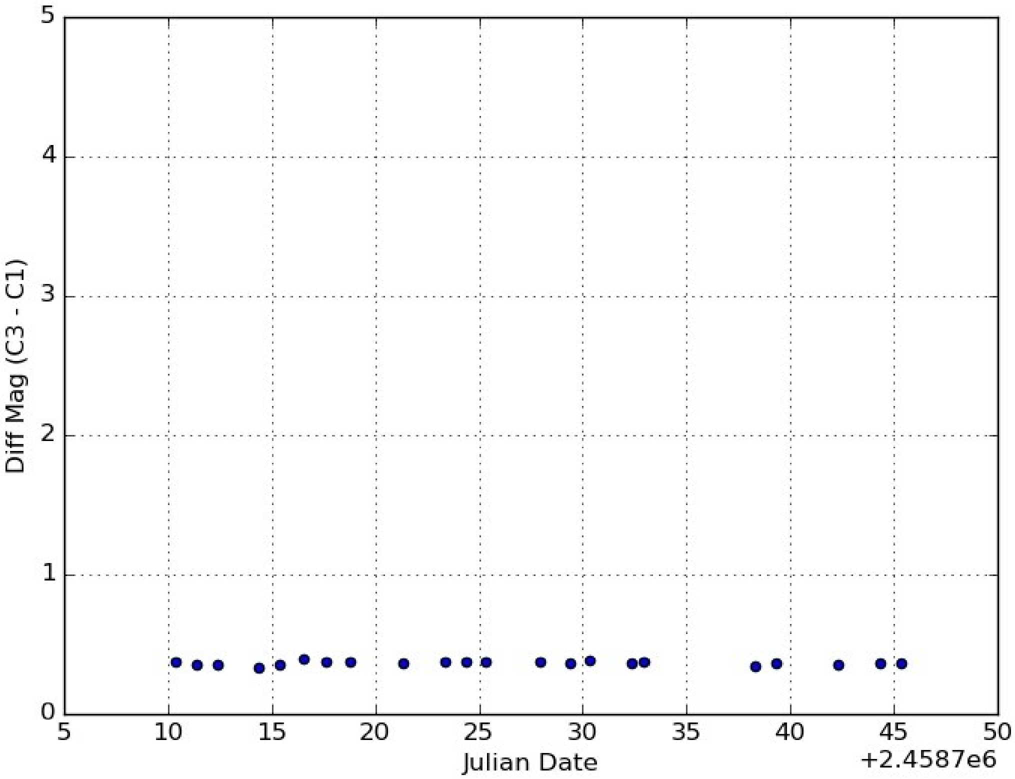

Fig 1.7: Light curve of differential magnitude between two comparison stars against Julian date

The clustering of the magnitude difference between the two comparison stars, (in figures 1.5, 1.6 and 1.7), demonstrates that neither of the comparison stars varied over the observation period. Their magnitude variations should be constant to provide a measurable value of the variable star.

Parallax = 0.0012131arcsec / 1.2131mas

d = 1/P

d = 1/0.001213 = 824.33435parsecs

1 parsec = 3.26ly = $3.0857*10^{16}$ m

824.33435 * $3.0857*10^{16}$ = $2.54365*10^{16}$ Km – distance to DW Cep

Period = 5.033804 days,

G = $6.6743*10^{11}$ $N.m^{2}$ $/Kg^{2}$

R = separation distance

Tangential velocity, $V_t = 4.7\mu d$ where μ is the proper motion of the star and d is the distance from Earth in parsecs

$\mu^2 = \mu_{RA}^2 - \mu_{Dec}^2$

μ_{RA} – 0.0050407 sec/yr

μ_{Dec} – 0.009218 arcsec/yr

μ = 0.07617, so that

$$Vt = 4.7*0.07617*824.33$$

$$= 295.11 Kms^{-1}$$

The tangential velocity is the component perpendicular to our line of sight . It is used to calculate the space velocity to describe how fast it is moving and in what direction. To get this, the component parallel to our line of sight, V_R radial velocity, must be known. This is not done in this project since the stars spectral line need to be measured to acquire the wavelength shift.

If an object subtends an angle θ and is at a distance, d, from the observer (telescope) and if θ is small as is always the case for objects in the sky, then the linear size of the object can be given by

$$D = \frac{\theta d}{206265}$$ where 206265 is the number of arcsecs in a circle / π

$$= \frac{0.001213 * 2.5437*10^{16} \text{ Km}}{206265}$$

$$= 149598905 \text{Km}$$

$$\approx 1.5 * 10^{8} \text{Km}$$

4.3 Error Analysis

Data is always susceptible to noise. Many methods for error analysis require knowledge about the noise distribution of the measured data. The easiest way to measure this error is to repeat a similar observation and monitor the distribution of the results. This can prove tough since considerable resources are needed (time, money, computational resources).

Some of the errors are likely to arise from:

- The data was collected during different times. The changes in atmospheric air mass, dust and mist could have scattered the light causing slight variations in the observable brightness of the star.
- Acquisition of perfect comparison stars was difficult since the binary system chosen does not have an existing AAVSO photometry chart to ease the process of selection.
- Systematic errors may have arisen during calculations and conversions to give slight differences from the true values.

CHAPTER 5: CONCLUSION

5.1 Conclusion

In this project we were able to select a binary star system from the catalogue and extract a light curve that shows the dips which represent the primary eclipse and the secondary eclipse to show that DW Cep is an eclipsing binary.

Our first objective was achieved by being able to select a binary system from the catalogue, the second objective was accomplished by being able to acquire data from the Las Cumbres Observatory, analyzing the data using the different software to get information easier to interpret and understand.

The third objective was achieved by acquiring plots from the data and we were able to get the dips showing the primary and secondary eclipses.

The final objective was cleared by estimating the orbital period, the diameter of the star and the tangential velocity of the star system.

5.2 Recommendations

With more resources, time and information base, future prospects on this subject include mapping out the mass, size, luminosity, temperature and chemical composition of the individual stars in the system. More data collection can also give us more accurate results about the period of the star and provide clarification on whether the system is truly an eclipsing binary or whether the results are greatly affected by systematic or statistical errors.

APPENDICES

CATALOGUE SELECTION

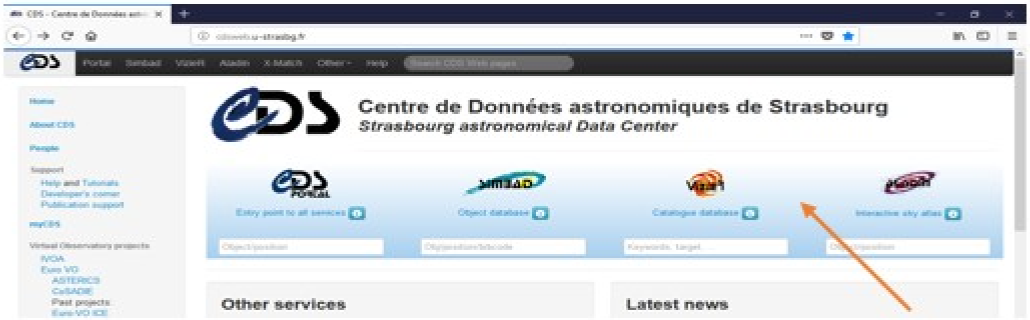

Figure 1

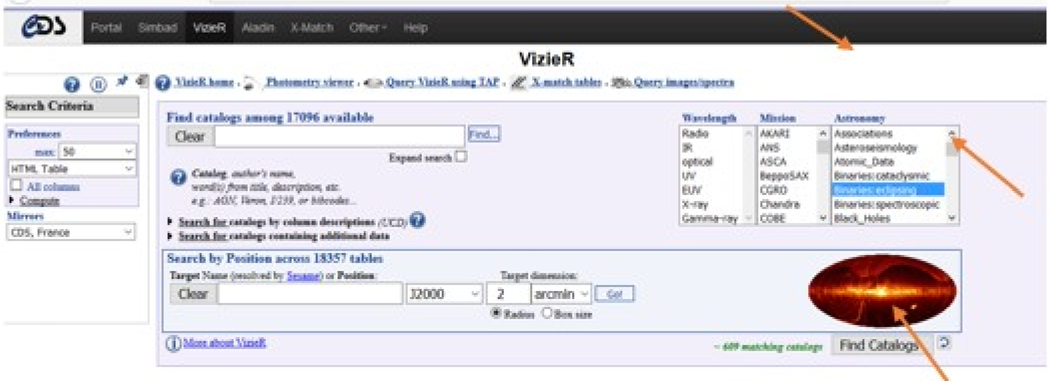

Figure 2

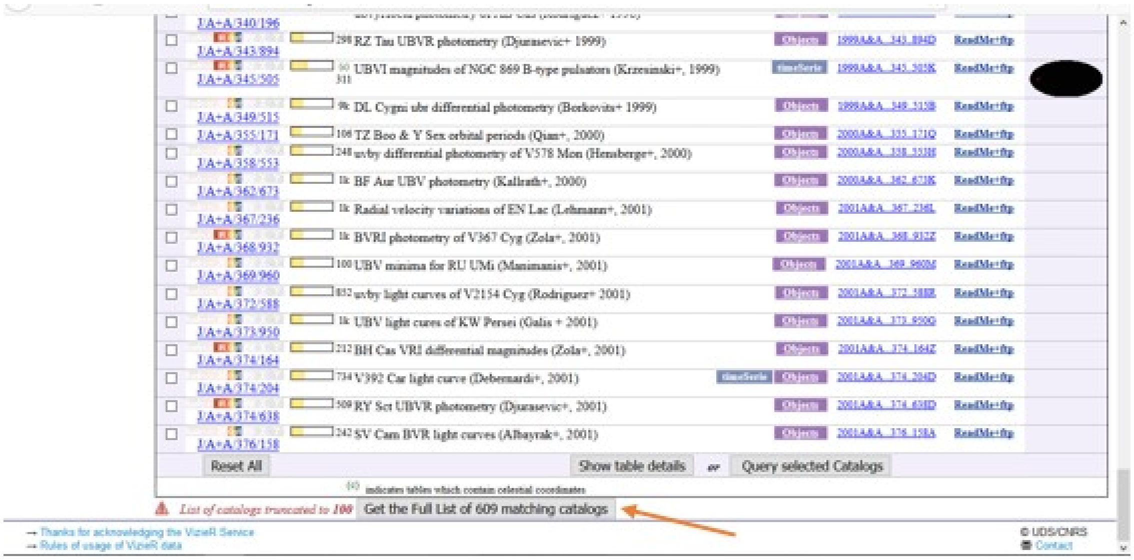

☐	J/A+A/343/894	298 RZ Tau UBVR photometry (Djurasevic+ 1999)		Objects	1999A&A...343..894D	ReadMe+ftp
☐	J/A+A/345/505	30 311 UBVI magnitudes of NGC 869 B-type pulsators (Krzesinski+, 1999)	timeSerie		1999A&A...345..505K	ReadMe+ftp
☐	J/A+A/349/515	9k DL Cygni uby differential photometry (Borkovits+ 1999)		Objects	1999A&A...349..515B	ReadMe+ftp
☐	J/A+A/355/171	108 TZ Boo & Y Sex orbital periods (Qian+, 2000)		Objects	2000A&A...355..171Q	ReadMe+ftp
☐	J/A+A/358/553	248 uvby differential photometry of V578 Mon (Hensberge+, 2000)		Objects	2000A&A...358..553H	ReadMe+ftp
☐	J/A+A/362/673	1k BF Aur UBV photometry (Kallrath+, 2000)		Objects	2000A&A...362..673K	ReadMe+ftp
☐	J/A+A/367/236	1k Radial velocity variations of EN Lac (Lehmann+, 2001)		Objects	2001A&A...367..236L	ReadMe+ftp
☐	J/A+A/368/932	1k BVRI photometry of V367 Cyg (Zola+, 2001)		Objects	2001A&A...368..932Z	ReadMe+ftp
☐	J/A+A/369/960	100 UBV minima for RU UMi (Manimanis+, 2001)		Objects	2001A&A...369..960M	ReadMe+ftp
☐	J/A+A/372/588	852 uvby light curves of V2154 Cyg (Rodriguez+ 2001)		Objects	2001A&A...372..588R	ReadMe+ftp
☐	J/A+A/373/950	1k UBV light cures of KW Persei (Galis + 2001)		Objects	2001A&A...373..950G	ReadMe+ftp
☐	J/A+A/374/164	212 BH Cas VRI differential magnitudes (Zola+, 2001)		Objects	2001A&A...374..164Z	ReadMe+ftp
☐	J/A+A/374/204	734 V392 Car light curve (Debernardi+, 2001)	timeSerie	Objects	2001A&A...374..204D	ReadMe+ftp
☐	J/A+A/374/638	509 RY Sct UBVR photometry (Djurasevic+, 2001)		Objects	2001A&A...374..638D	ReadMe+ftp
☐	J/A+A/376/158	242 SV Cam BVR light curves (Albayrak+, 2001)		Objects	2001A&A...376..158A	ReadMe+ftp

[redacted]

Figure 3

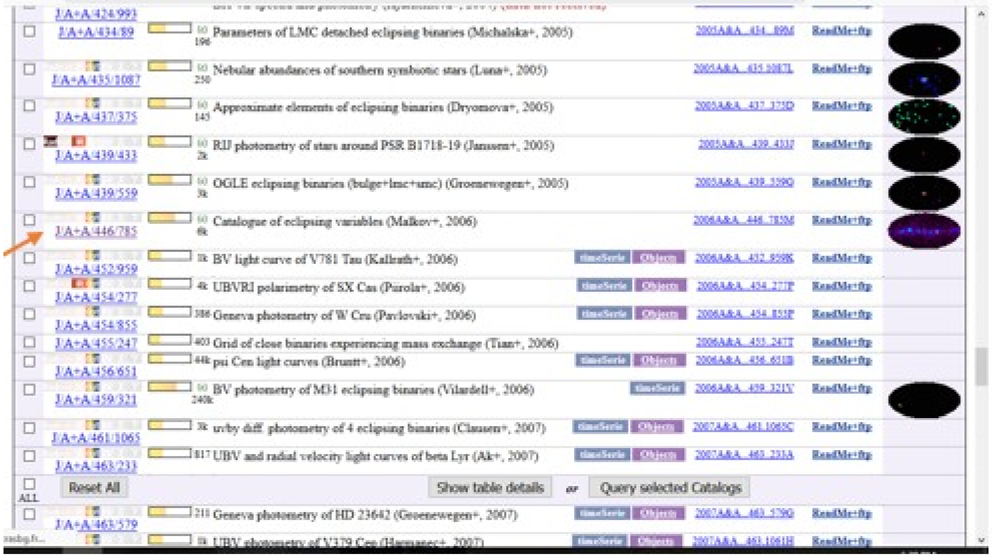

	Catalogue	Size	Title	Bibcode	
☐	J/A+A/424/993				
☐	J/A+A/434/89	196	Parameters of LMC detached eclipsing binaries (Michalska+, 2005)	2005A&A...434..89M	ReadMe+ftp
☐	J/A+A/435/1087	250	Nebular abundances of southern symbiotic stars (Luna+, 2005)	2005A&A...435.1087L	ReadMe+ftp
☐	J/A+A/437/375	143	Approximate elements of eclipsing binaries (Dryomova+, 2005)	2005A&A...437..375D	ReadMe+ftp
☐	J/A+A/439/433	2k	RIJ photometry of stars around PSR B1718-19 (Janssen+, 2005)	2005A&A...439..433J	ReadMe+ftp
☐	J/A+A/439/559	3k	OGLE eclipsing binaries (bulge+lmc+smc) (Groenewegen+, 2005)	2005A&A...439..559G	ReadMe+ftp
☐	J/A+A/446/785	6k	Catalogue of eclipsing variables (Malkov+, 2006)	2006A&A...446..785M	ReadMe+ftp
☐	J/A+A/452/959	1k	BV light curve of V781 Tau (Kalluth+, 2006) timeSerie Objects	2006A&A...452..959K	ReadMe+ftp
☐	J/A+A/454/277	4k	UBVRI polarimetry of SX Cas (Piirola+, 2006) timeSerie Objects	2006A&A...454..277P	ReadMe+ftp
☐	J/A+A/454/855	386	Geneva photometry of W Cru (Pavlovski+, 2006) timeSerie Objects	2006A&A...454..855P	ReadMe+ftp
☐	J/A+A/455/247	403	Grid of close binaries experiencing mass exchange (Tian+, 2006)	2006A&A...455..247T	ReadMe+ftp
☐	J/A+A/456/651	44k	psi Cen light curves (Bruntt+, 2006) timeSerie Objects	2006A&A...456..651B	ReadMe+ftp
☐	J/A+A/459/321	240k	BV photometry of M31 eclipsing binaries (Vilardell+, 2006) timeSerie	2006A&A...459..321V	ReadMe+ftp
☐	J/A+A/461/1065	3k	uvby diff. photometry of 4 eclipsing binaries (Clausen+, 2007) timeSerie Objects	2007A&A...461.1065C	ReadMe+ftp
☐	J/A+A/463/233	817	UBV and radial velocity light curves of beta Lyr (Ak+, 2007) timeSerie Objects	2007A&A...463..233A	ReadMe+ftp
☐ ALL	Reset All		Show table details or Query selected Catalogs		
☐	J/A+A/463/579	211	Geneva photometry of HD 23642 (Groenewegen+, 2007) timeSerie Objects	2007A&A...463..579G	ReadMe+ftp
		1k	UBV photometry of V379 Cen (Harmanec+, 2007) timeSerie Objects	2007A&A...463.1061H	ReadMe+ftp

Figure 4

SELECTING ECLIPSING BINARY IN CATALOGUE

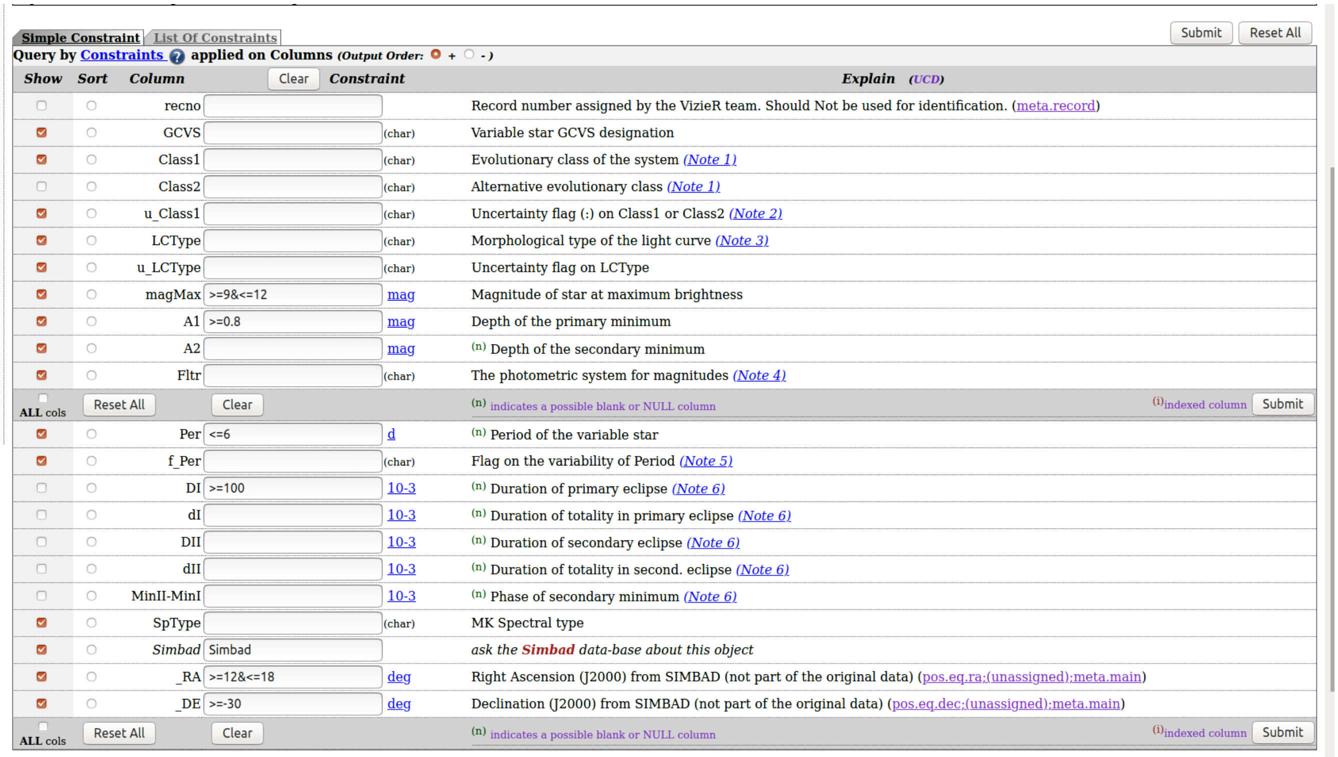

Query by Constraints applied on Columns *(Output Order: ● + ○ -)*

Show	Sort	Column	Constraint		Explain (UCD)
☐	○	recno			Record number assigned by the VizieR team. Should Not be used for identification. (meta.record)
☑	○	GCVS		(char)	Variable star GCVS designation
☑	○	Class1		(char)	Evolutionary class of the system (Note 1)
☐	○	Class2		(char)	Alternative evolutionary class (Note 1)
☑	○	u_Class1		(char)	Uncertainty flag (:) on Class1 or Class2 (Note 2)
☑	○	LCType		(char)	Morphological type of the light curve (Note 3)
☑	○	u_LCType		(char)	Uncertainty flag on LCType
☑	○	magMax	>=9&<=12	mag	Magnitude of star at maximum brightness
☑	○	A1	>=0.8	mag	Depth of the primary minimum
☑	○	A2		mag	(n) Depth of the secondary minimum
☑	○	Fltr		(char)	The photometric system for magnitudes (Note 4)
☐ ALL cols	Reset All		Clear		(n) indicates a possible blank or NULL column (i)indexed column Submit
☑	○	Per	<=6	d	(n) Period of the variable star
☑	○	f_Per		(char)	Flag on the variability of Period (Note 5)
☐	○	DI	>=100	10-3	(n) Duration of primary eclipse (Note 6)
☐	○	dI		10-3	(n) Duration of totality in primary eclipse (Note 6)
☐	○	DII		10-3	(n) Duration of secondary eclipse (Note 6)
☐	○	dII		10-3	(n) Duration of totality in second. eclipse (Note 6)
☐	○	MinII-MinI		10-3	(n) Phase of secondary minimum (Note 6)
☑	○	SpType		(char)	MK Spectral type
☑	○	*Simbad*	Simbad		*ask the* ***Simbad*** *data-base about this object*
☑	○	_RA	>=12&<=18	deg	Right Ascension (J2000) from SIMBAD (not part of the original data) (pos.eq.ra;(unassigned);meta.main)
☑	○	_DE	>=-30	deg	Declination (J2000) from SIMBAD (not part of the original data) (pos.eq.dec;(unassigned);meta.main)
☐ ALL cols	Reset All		Clear		(n) indicates a possible blank or NULL column (i)indexed column Submit

Figure 5

DATA COLLECTION FROM LCO WEBSITE

Figure 6

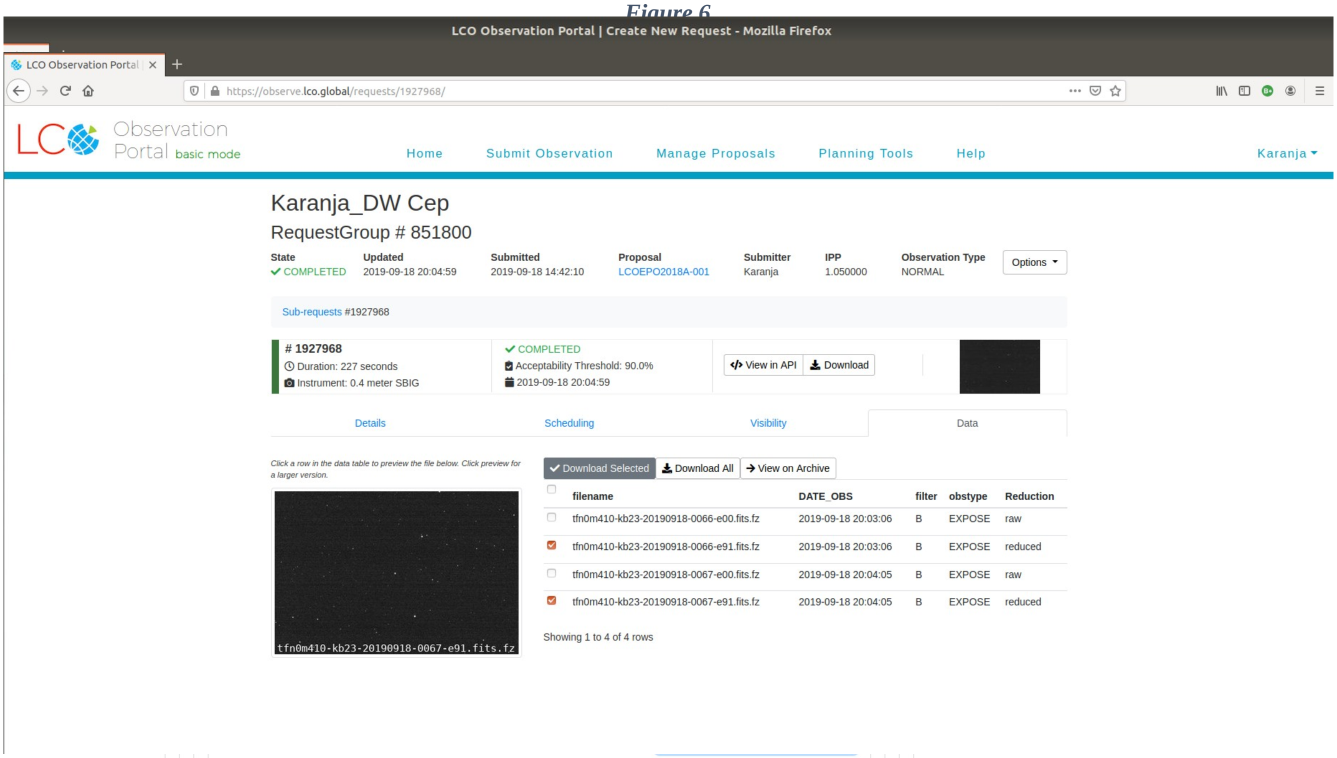

Karanja_DW Cep

RequestGroup # 851800

State	Updated	Submitted	Proposal	Submitter	IPP	Observation Type
✓ COMPLETED	2019-09-18 20:04:59	2019-09-18 14:42:10	LCOEPO2018A-001	Karanja	1.050000	NORMAL

Sub-requests #1927968

1927968
Duration: 227 seconds
Instrument: 0.4 meter SBIG

✓ COMPLETED
Acceptability Threshold: 90.0%
2019-09-18 20:04:59

Click a row in the data table to preview the file below. Click preview for a larger version.

☐	filename	DATE_OBS	filter	obstype	Reduction
☐	tfn0m410-kb23-20190918-0066-e00.fits.fz	2019-09-18 20:03:06	B	EXPOSE	raw
☑	tfn0m410-kb23-20190918-0066-e91.fits.fz	2019-09-18 20:03:06	B	EXPOSE	reduced
☐	tfn0m410-kb23-20190918-0067-e00.fits.fz	2019-09-18 20:04:05	B	EXPOSE	raw
☑	tfn0m410-kb23-20190918-0067-e91.fits.fz	2019-09-18 20:04:05	B	EXPOSE	reduced

Showing 1 to 4 of 4 rows

Sexagesimal: 20:51:39.6899
Right Ascension ? 312.9153746796436

Sexagesimal: 62:48:50.2927
Declination ? 62.8139701926639

IDENTIFICATION OF COMPARISON STARS

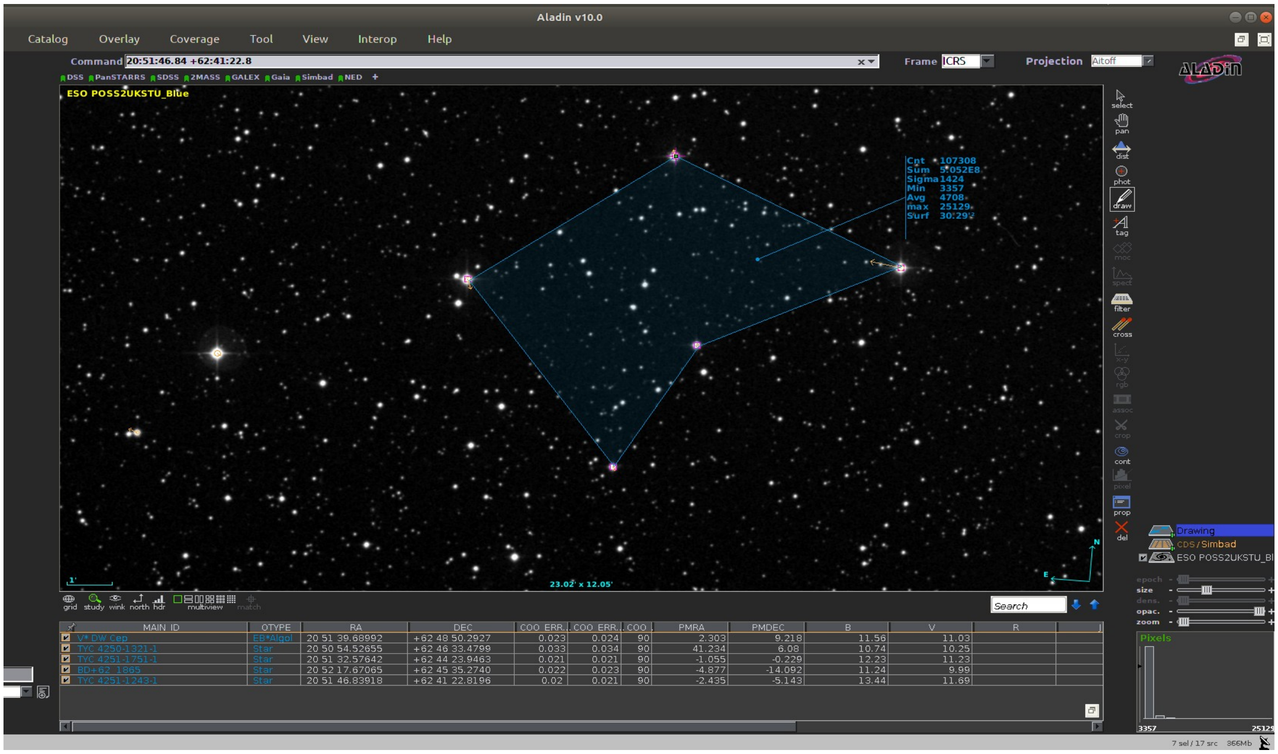

MAIN_ID	OTYPE	RA	DEC	COO_ERR...	COO_ERR...	COO	PMRA	PMDEC	B	V	R
V* DW Cep	EB*Algol	20 51 39.68992	+62 48 50.2927	0.023	0.024	90	2.303	9.218	11.56	11.03	
TYC 4250-1321-1	Star	20 50 54.52655	+62 46 33.4799	0.033	0.034	90	41.234	6.08	10.74	10.25	
TYC 4251-1751-1	Star	20 51 32.57642	+62 44 23.9463	0.021	0.021	90	-1.055	-0.229	12.23	11.23	
BD+62 1865	Star	20 52 17.67065	+62 45 35.2740	0.022	0.023	90	-4.877	-14.092	11.24	9.99	
TYC 4251-1243-1	Star	20 51 46.83918	+62 41 22.8196	0.02	0.021	90	-2.435	-5.143	13.44	11.69	

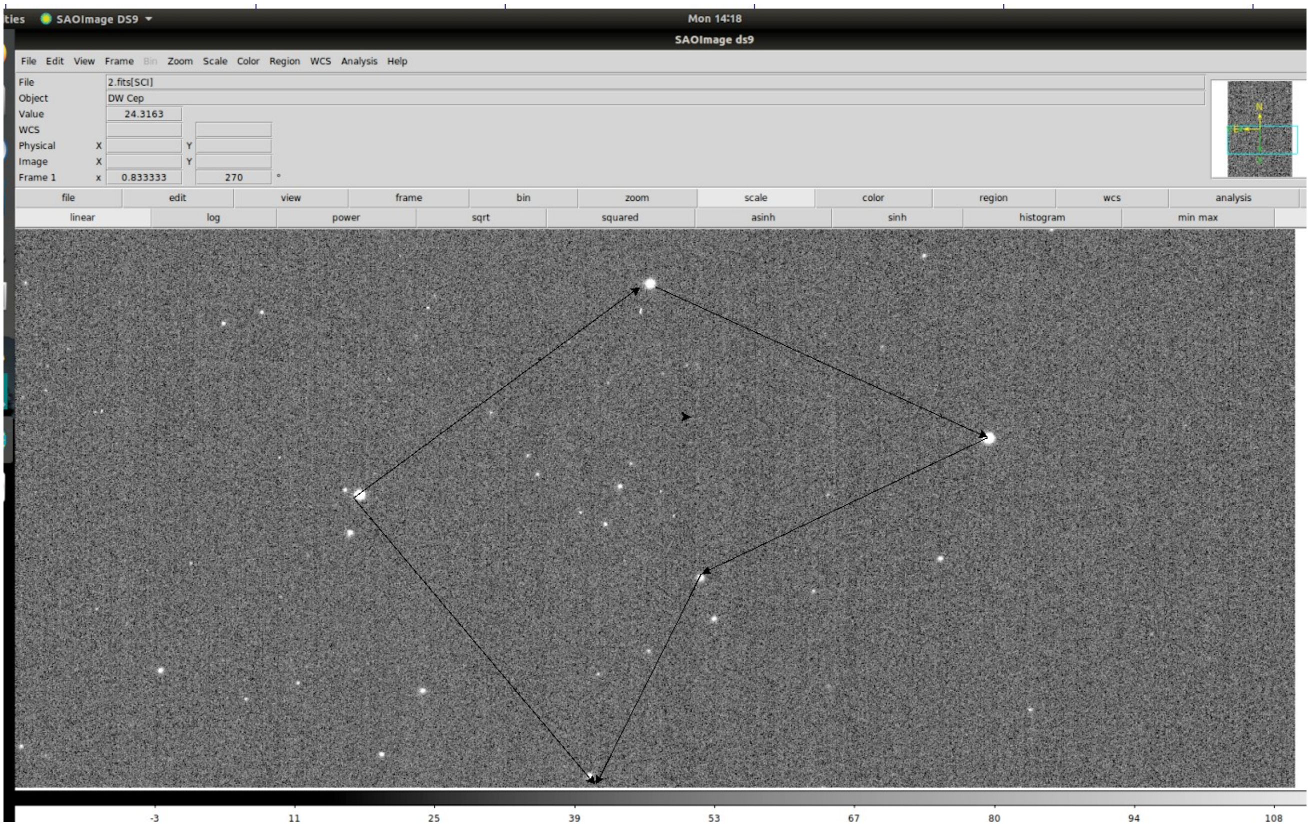

File 2.fits[SCI]
Object DW Cep
Value 24.3163
WCS
Physical X Y
Image X Y
Frame 1 x 0.833333 270 °

Figure 9

IMAGE SPECS IDENTIFICATION

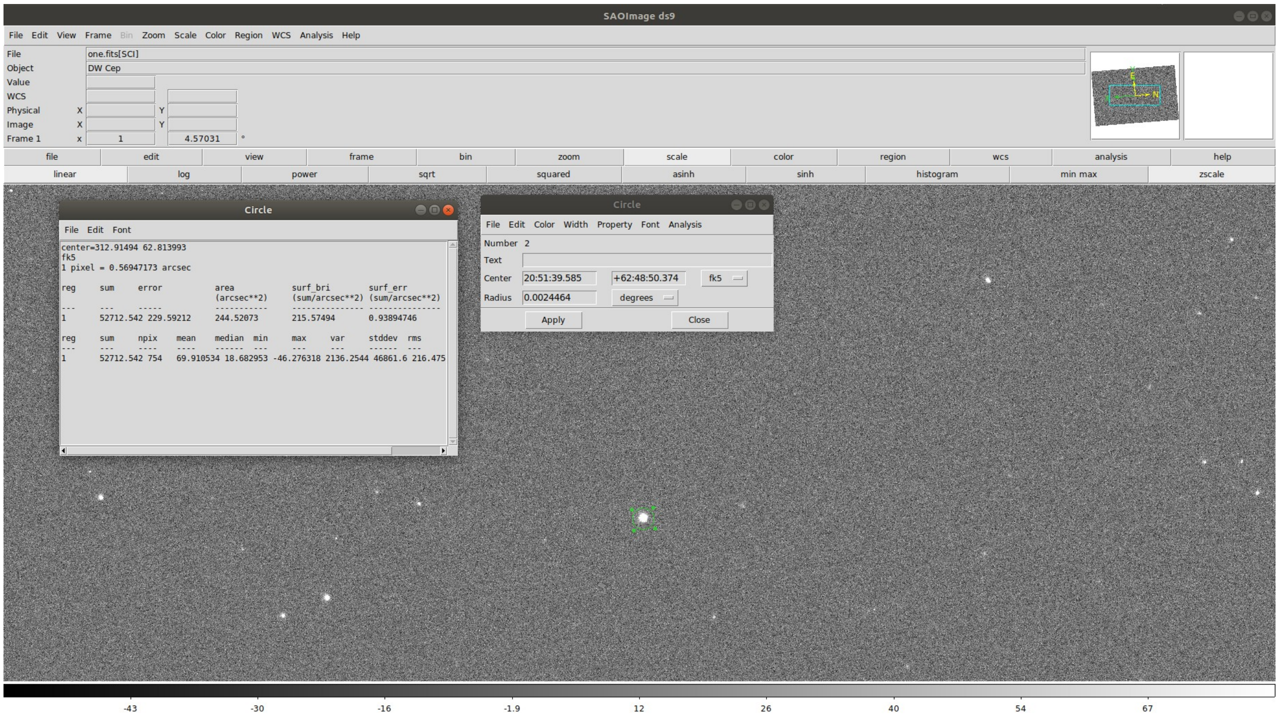

File one.fits[SCI]
Object DW Cep
Value
WCS
Physical X Y
Image X Y
Frame 1 x 1 4.57031 °

```
center=312.91494 62.813993
fk5
1 pixel = 0.56947173 arcsec

reg     sum     error           area            surf_bri        surf_err
                                (arcsec**2)     (sum/arcsec**2) (sum/arcsec**2)
---     ---     -----           -----------     --------------- ---------------
1       52712.542 229.59212     244.52073       215.57494       0.93894746

reg     sum     npix    mean    median  min     max     var     stddev  rms
---     ---     ----    ----    ------  ---     ---     ---     ------  ---
1       52712.542 754   69.910534 18.682953 -46.276318 2136.2544 46861.6 216.475
```

Number 2
Text
Center 20:51:39.585 +62:48:50.374 fk5
Radius 0.0024464 degrees

Figure 10

IRIS AUTOMATIC APERTURE PHOTOMETRY

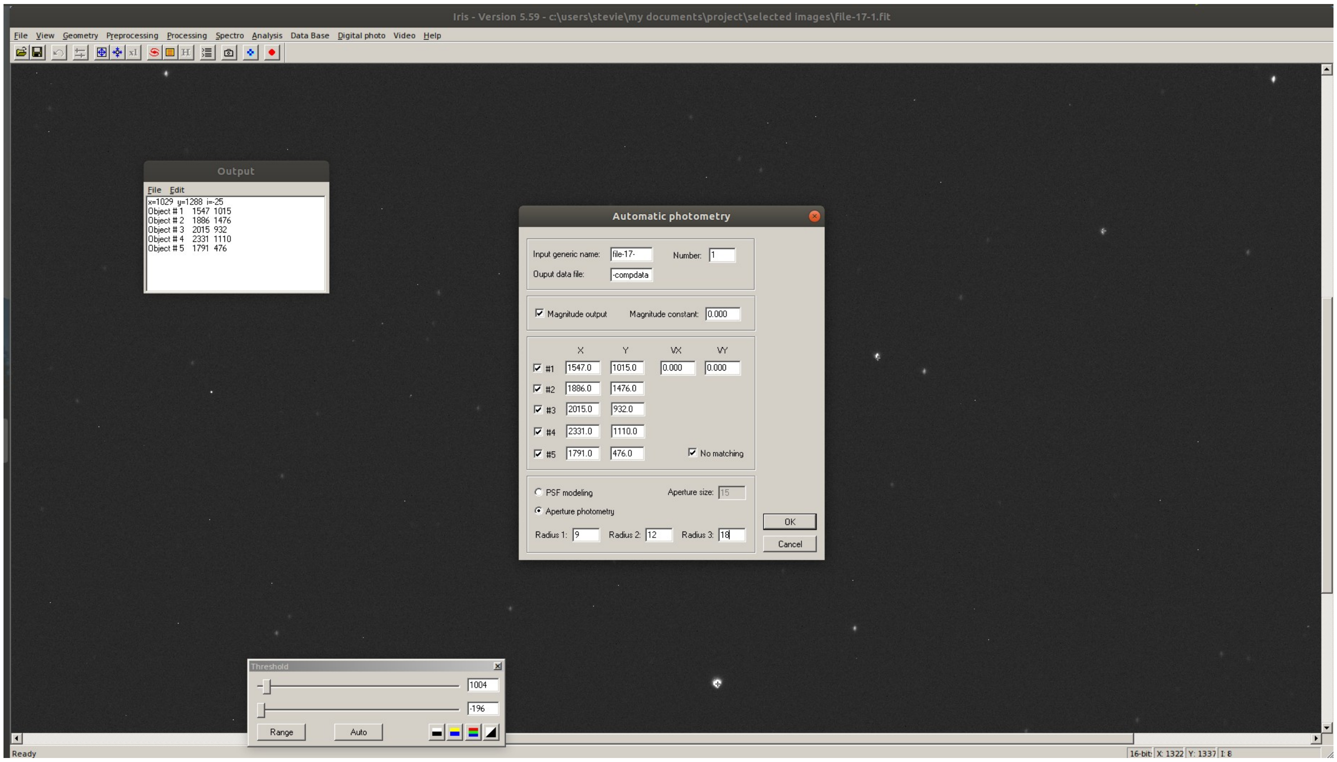

```
x=1029  y=1288  i=-25
Object # 1   1547  1015
Object # 2   1886  1476
Object # 3   2015  932
Object # 4   2331  1110
Object # 5   1791  476
```

Input generic name: file-17- Number: 1
Ouput data file: -compdata

☑ Magnitude output Magnitude constant: 0.000

	X	Y	VX	VY
☑ #1	1547.0	1015.0	0.000	0.000
☑ #2	1886.0	1476.0		
☑ #3	2015.0	932.0		
☑ #4	2331.0	1110.0		
☑ #5	1791.0	476.0		

☑ No matching

○ PSF modeling Aperture size: 15
● Aperture photometry
Radius 1: 9 Radius 2: 12 Radius 3: 18

Threshold: 1004 -196

16-bit: X: 1322 Y: 1337 I: 8

Figure 11

EXCEL COMPUTATION

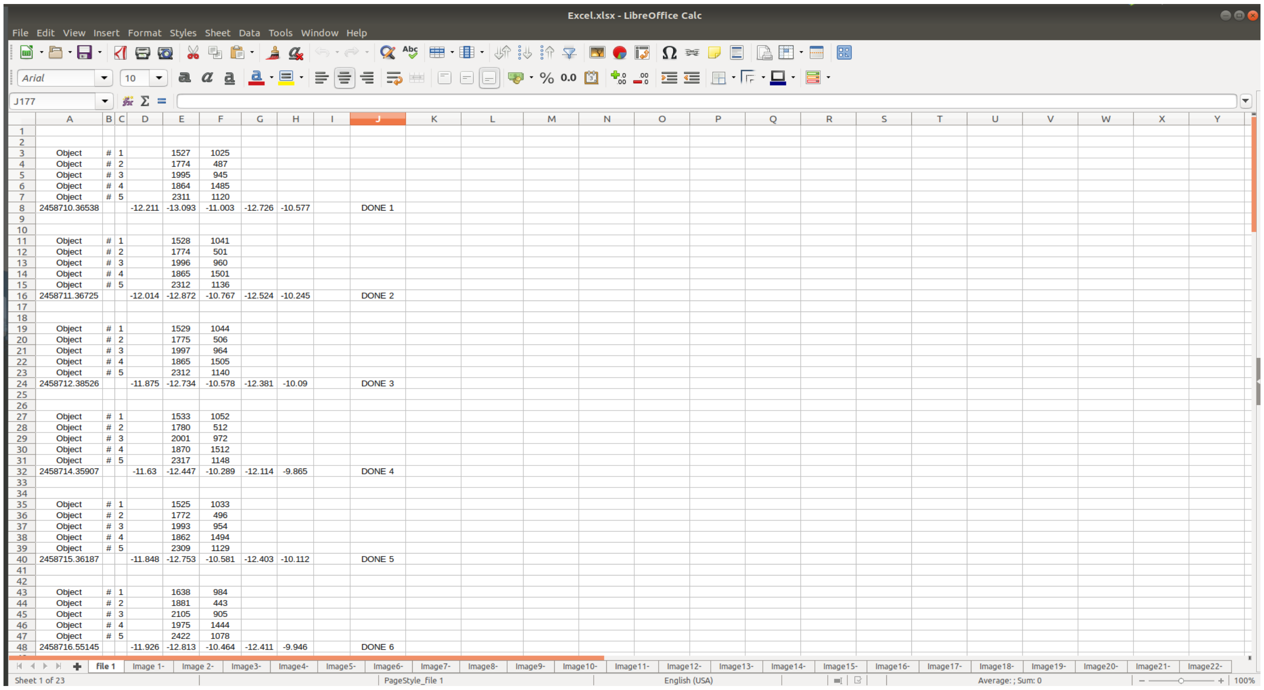

	A	B	C	D	E	F	G	H	I	J
1										
2										
3	Object	#	1		1527	1025				
4	Object	#	2		1774	487				
5	Object	#	3		1995	945				
6	Object	#	4		1864	1485				
7	Object	#	5		2311	1120				
8	2458710.36538			-12.211	-13.093	-11.003	-12.726	-10.577		DONE 1
9										
10										
11	Object	#	1		1528	1041				
12	Object	#	2		1774	501				
13	Object	#	3		1996	960				
14	Object	#	4		1865	1501				
15	Object	#	5		2312	1136				
16	2458711.36725			-12.014	-12.872	-10.767	-12.524	-10.245		DONE 2
17										
18										
19	Object	#	1		1529	1044				
20	Object	#	2		1775	506				
21	Object	#	3		1997	964				
22	Object	#	4		1865	1505				
23	Object	#	5		2312	1140				
24	2458712.38526			-11.875	-12.734	-10.578	-12.381	-10.09		DONE 3
25										
26										
27	Object	#	1		1533	1052				
28	Object	#	2		1780	512				
29	Object	#	3		2001	972				
30	Object	#	4		1870	1512				
31	Object	#	5		2317	1148				
32	2458714.35907			-11.63	-12.447	-10.289	-12.114	-9.865		DONE 4
33										
34										
35	Object	#	1		1525	1033				
36	Object	#	2		1772	496				
37	Object	#	3		1993	954				
38	Object	#	4		1862	1494				
39	Object	#	5		2309	1129				
40	2458715.36187			-11.848	-12.753	-10.581	-12.403	-10.112		DONE 5
41										
42										
43	Object	#	1		1638	984				
44	Object	#	2		1881	443				
45	Object	#	3		2105	905				
46	Object	#	4		1975	1444				
47	Object	#	5		2422	1078				
48	2458716.55145			-11.926	-12.813	-10.464	-12.411	-9.946		DONE 6

Figure 12

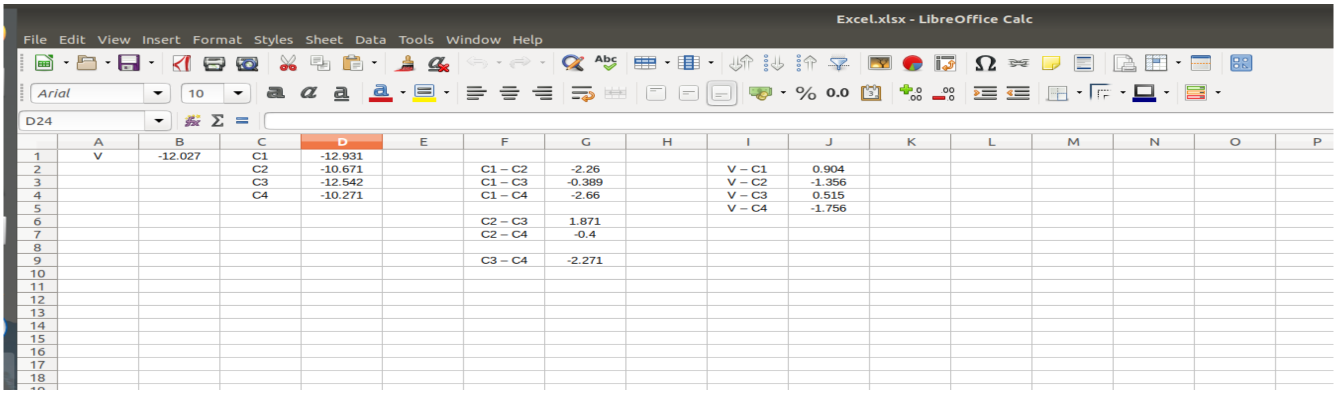

	A	B	C	D	E	F	G	H	I	J
1	V	-12.027	C1	-12.931						
2			C2	-10.671		C1 – C2	-2.26		V – C1	0.904
3			C3	-12.542		C1 – C3	-0.389		V – C2	-1.356
4			C4	-10.271		C1 – C4	-2.66		V – C3	0.515
5									V – C4	-1.756
6						C2 – C3	1.871			
7						C2 – C4	-0.4			
8										
9						C3 – C4	-2.271			

Figure 13

Python Computations

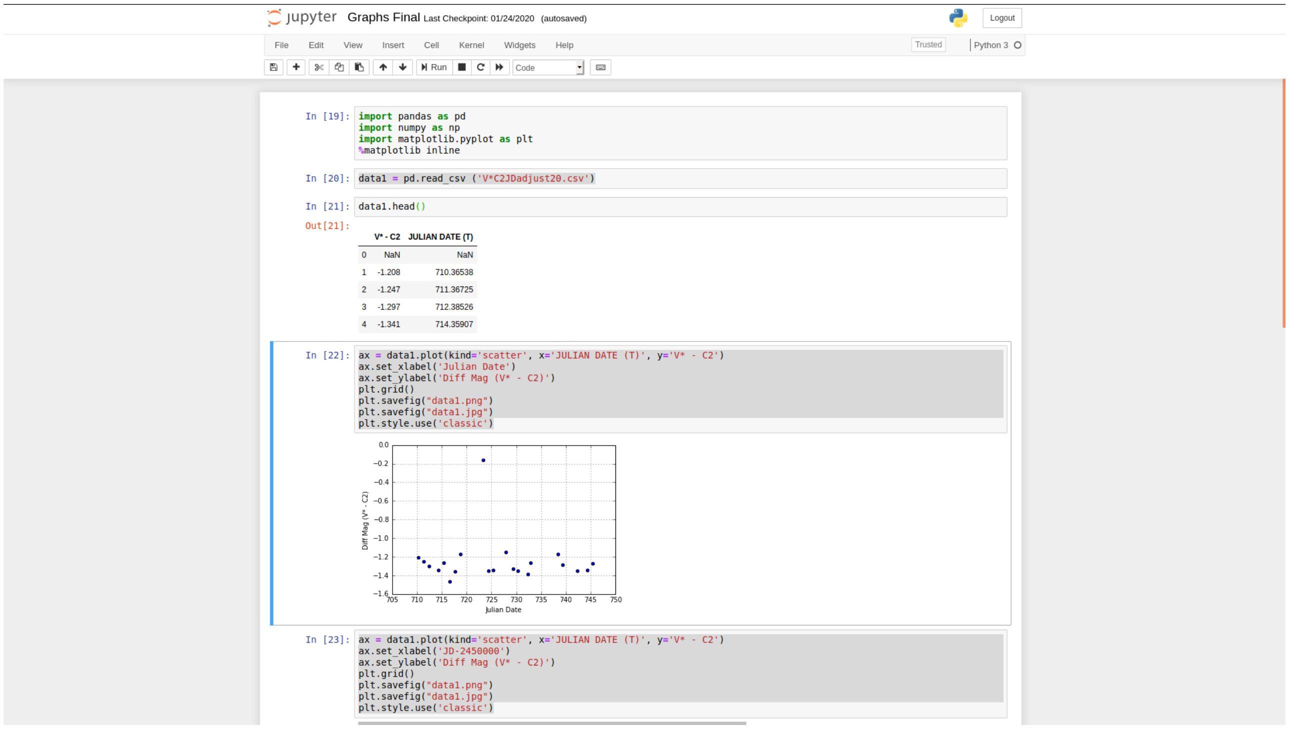

```
In [19]: import pandas as pd
         import numpy as np
         import matplotlib.pyplot as plt
         %matplotlib inline

In [20]: data1 = pd.read_csv ('V*C2JDadjust20.csv')

In [21]: data1.head()

Out[21]:
```

	V* - C2	JULIAN DATE (T)
0	NaN	NaN
1	-1.208	710.36538
2	-1.247	711.36725
3	-1.297	712.38526
4	-1.341	714.35907

```
In [22]: ax = data1.plot(kind='scatter', x='JULIAN DATE (T)', y='V* - C2')
         ax.set_xlabel('Julian Date')
         ax.set_ylabel('Diff Mag (V* - C2)')
         plt.grid()
         plt.savefig("data1.png")
         plt.savefig("data1.jpg")
         plt.style.use('classic')
```

```
In [23]: ax = data1.plot(kind='scatter', x='JULIAN DATE (T)', y='V* - C2')
         ax.set_xlabel('JD-2450000')
         ax.set_ylabel('Diff Mag (V* - C2)')
         plt.grid()
         plt.savefig("data1.png")
         plt.savefig("data1.jpg")
         plt.style.use('classic')
```

Fig 14

Bibliography

1. P. B. Demorest et al., A two-solar-mass neutron star measured using Shapiro delay, Nature 467, 1081 (2010)

2.G. Torres, J. Andersen, A. Gimenez, Accurate masses and radii of normal stars: modern results and applications, Astron. Astrophys. Rev, 18, 67-126 (2010) arXiv:0908.2624v1

3. Niemela V s. A Short History and other Stories of Binary Stars. Rev Mex Astron y Astrofísica. 2001;11(June):23–6.

4. Price A. American Association of Variable Star Observers [Internet]. Available from: https://www.aavso.org/vsots_betaper

5. Michell J. An Inquiry into the Probable Parallax, and Magnitude of the Fixed Stars, from the Quantity of Light Which They Afford us, and the Particular Circumstances of Their Situation. Philos Trans. 1767;57:234–64.

6.http://www.etsu.edu/physics/ignace/binaries.html (5.11.2010)

7. Kutner ML. Astronomy A Physical Perspective. Second. 2003.

8.A. Prsa et al., Kepler Eclipsing Binary Stars. I. Catalog and Principal Characterization of 1832 Eclipsing Binaries in the First Data Release, arXiv/astro-ph, arXiv:1006.2815v1

9. A. Tokovinin, Statistics of multiple stars, RevMexAA (Serie de Conferencias), Vol 21,7-14 (2004)

10. Zinnecker H, Mathieu RD. The Formation of Binary Stars. In.

11. Sahade J, McCluskey Jr. GE, Kondo Y. The Realm of Interracting Binary Stars. Kluwer Academic Publishers; 1993.

12. Tohline J ~E. The Origin of Binary Stars. Annu Rev Astron Astrophys. 2002;40:349–85.

*13. Benacquista M. An Introduction to the Evolution of Single and Binary Stars. Springer;
2012.*

14. Bodenheimer PH. Principles of Star Formation. Principles of Star Formation: Springer;
2011.11
15. Bonnell I a., Bate MR. The Formation of Close Binary Systems. Mon Not R Astron Soc [Internet]. 1994;271:999–1004. Available from:
http://adsabs.harvard.edu/abs/1994MNRAS.271..999B

16. Tohline JE, Cazes JE, Cohl HS. The Formation of Common-Envelope, Pre-Main-Sequence Binary Stars [Internet]. Available from:
http://www.phys.lsu.edu/astro/nap98/bf.final.html

17. Brainerd JJ. Theories of the Birth Of Binary Stars [Internet]. Available from:
http://www.astrophysicsspectator.com/topics/stars/BinaryStarBirth.html

18. Durisen RH, Gingold RA, Tohline JE, Boss AP. Dynamic fission instabilities in rapidly rotating N = 3/2 polytropes - A comparison of results from finite-difference and smoothed particle hydrodynamics codes. Astrophys J. 1986;305:281–308.

19. Tobin JJ, Chandler CJ, Wilner DJ, Looney LW, Loinard L, Chiang H-F, et al. VLA and CARMA Observations of Protostars in the Cepheus Clouds: Sub-arcsecond Proto-binaries Formed via Disk Fragmentation. Astrophys J [Internet]. 2013;779(2):93.

20. Offner SSR, Kratter KM, Matzner CD, Krumholz MR, Klein RI. The Formation of Low-Mass Binary Star Systems Via Turbulent Fragmentation. Astrophys J [Internet]. 2010;725(2):1485–94. Available from: http://stacks.iop.org/0004-637X/725/i=2/a=1485?key=crossref.9fd96275c951e2bc4784e8df0e3ea8f4

21. Iben, Jr I, Livio M. Common Envelopes In Binary Star Evolution. Astron Soc Pacific.
1993;105(694):1373–406.

22. Hurley JR, Tout C a., Pols OR. Evolution of binary stars and the effect of tides on binary populations. Mon Not R Astron Soc. 2002;329(4):897–926.